Thermal conductivity anisotropy in a ferromagnetic superconductor, UGe_2

2005 J. Phys.: Condens. Matter 17 679

(http://iopscience.iop.org/0953-8984/17/4/010)

INSTITUTE OF PHYSICS PUBLISHING JOURNAL OF PHYSICS: CONDENSED MATTER

J. Phys.: Condens. Matter **17** (2005) 679–688 doi:10.1088/0953-8984/17/4/010

Thermal conductivity anisotropy in a ferromagnetic superconductor, UGe_2

H Misiorek[1], J Mucha[1], R Troć[1] and B Coqblin[2]

[1] W Trzebiatowski Institute of Low Temperature and Structure Research, Polish Academy of Sciences, PO Box 1410, 50-950 Wrocław 2, Poland
[2] Laboratoire de Physique des Solides, Bâtiment 510, Université Paris-Sud, 91405 Orsay, France

E-mail: troc@int.pan.wroc.pl

Received 22 September 2004, in final form 6 December 2004
Published 14 January 2005
Online at stacks.iop.org/JPhysCM/17/679

Abstract

We report on the first measurements of the anisotropy of the thermal conductivity of a single crystal of the ferromagnetic superconductor UGe_2, with the heat current applied parallel to the three orthorhombic main axes of the unit cell. The thermal conductivity was measured over the temperature range 4.2–300 K. The results obtained are discussed in the framework of various contributions to the total thermal conductivity of magnetically ordered material. As a reference compound, polycrystalline $ThGe_2$ has been used.

1. Introduction

The discovery of superconductivity (SC) under pressure in ferromagnetic UGe_2 ($T_C = 53$ K and $\mu_S \approx 1.4\,\mu_B$ at ambient pressure) [1] is still associated with the observation of a broad anomaly in the temperature derivative of the resistivity having a maximum at the so-called characteristic temperature T^*, first reported by Oomi *et al* [2]. An anomaly at T^* was also clearly detected in the coefficient of volume thermal expansion α_V [3]. This temperature at ambient pressure is around 30 K and just reaches zero at the critical pressure $p_C^* \approx 12$ kbar, where T_{SC} becomes the highest (0.8 K) [1]. At the same pressure, $T_C = 32$ K and $\mu_S = 1\,\mu_B$, and the ferromagnetism (FM) disappears at the QCP, where the critical pressure is $p_C \approx 16$ kbar. Until now, the nature of the characteristic temperature T^* has been a matter of intensive debate in the literature. Most of the works devoted to the coexistence of SC and FM in UGe_2 have been focused so far on the electronic and magnetic properties of this compound under pressure. It is natural to think, however, that the reason for the occurrence of SC in UGe_2 under pressure is certainly connected with its properties at ambient pressure. The first magnetization measurement on a single-crystalline sample of UGe_2 was performed by Menovsky *et al* [4], who found a huge anisotropic behaviour with the easy magnetization along axis **a**.

Recently, we have discovered around T^* an unusual temperature dependence of the transverse magnetoresistivity (TMR), first for polycrystalline [5] and then for single-crystalline [6] UGe_2 samples. The TMR measured for a UGe_2 single crystal along the three

main axes was found to be highly anisotropic. At low temperature the TMR for the **a**, **b** and **c** axes is positive and its magnitudes at 4.2 K and 8 T are in the following proportions: 1:4:2 (respectively). It should be mentioned here that in the orthorhombic crystal structure of the $ZrGa_2$ type (space group $Cmmm$) in which UGe_2 crystallizes [7], the lattice parameter b/a ratio is as large as 3.75. This clearly shows that the smallest effect in TMR is for cases where the current **j** flows along the easy axis **a** and the largest one is for the hardest direction, **b**. At temperatures above about 15 K (**b** axis) and 25 K (**a** and **c** axes) the TMR becomes negative with a minimum at T_C, as one would expect for a ferromagnet, but only for the latter two directions. However, the most spectacular behaviour is observed when the current $\mathbf{j} \parallel \mathbf{b}$ and the magnetic field $\mathbf{B} \parallel \mathbf{a}$. For this configuration the TMR goes through a very broad negative minimum where it reaches a value of about -40% at $T = 27$ K, i.e. at a temperature close to the characteristic temperature T^*. Therefore, this effect in TMR can be considered as the most distinct and peculiar manifestation of some kind of strong magnetic fluctuations in UGe_2, but taking place in the ferromagnetic ordering just at the temperature $T_{sf} \approx T_C/2$, close to T^*, but surprisingly without an apparent manifestation at T_C.

In this work, detailed data are given for the thermal conductivity properties of UGe_2 determined at ambient pressure for a single-crystalline sample. We have tried to relate these properties to a non-magnetic isostructural reference compound. However, our sample of $ThGe_2$ displayed an orthorhombic crystal structure of $ZrSi_2$ type (space group $Cmcm$) [8], not exactly isomorphic to the UGe_2 one. However, the two structures show a close relationship and can be interconverted by a simple crystallographic translation [8].

2. Experimental details

The oriented UGe_2 single crystals, of $1 \times 1 \times 5$ mm^3 dimensions, were cut off from a bigger one obtained by the Czochralski method. The lattice parameters were as published before, in [6]. The $ThGe_2$ sample was obtained by arc melting the components under an argon atmosphere and then annealing the sample at 800 °C for 30 days. The x-ray pattern showed only one phase of the orthorhombic $ZrSi_2$-type structure with the following lattice parameters: $\mathbf{a} = 0.4028(1)$, $\mathbf{b} = 0.4146(1)$ and $\mathbf{c} = 1.6624(5)$ nm.

The thermal conductivity measurements were performed using the stationary heat flux method in the temperature range 4.2–300 K. The experimental set-up and the procedure have been described in detail in [9]. The sample temperature was measured with a constantan–manganin thermocouple, with liquid nitrogen and liquid helium temperatures as reference points. The temperature difference along the sample was 0.2 K. The time of temperature stabilization between two consecutive experimental points was 1 h above 78 K, decreasing to 15 min at temperatures of about 10 K. Particular care was taken to avoid parasitic heat transfer between the sample and its environment. The sample was placed inside a cylindrical screen, along which the temperature gradient was identical with that along the sample. The mean temperatures of the sample and the screen were also identical. All current and voltage leads were thermally anchored to the screen. The measurement error was below $\pm 3\%$ and the surplus error, estimated from the scatter in the measurement points, did not exceed $\pm 0.2\%$.

The electrical resistivity of the same samples was measured [6] and the results have been used to calculate the electronic part of the thermal conductivity of UGe_2.

3. Experimental results

The results on the measured thermal conductivity of UGe_2 versus temperature for the **a**, **b** and **c** crystallographic axes are displayed in figure 1; on the same figure, we have also plotted

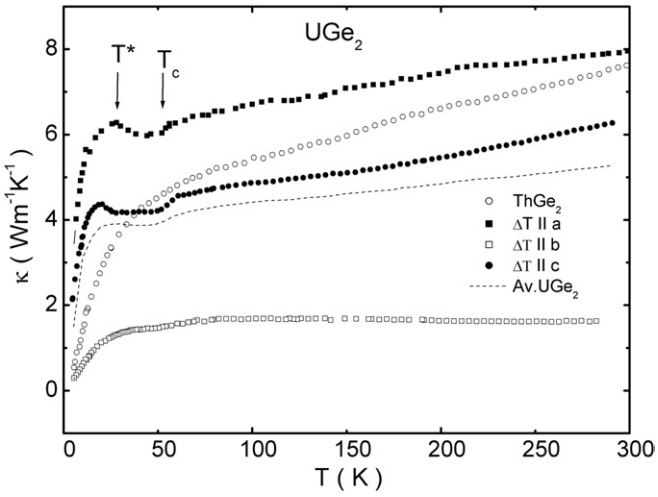

Figure 1. The total thermal conductivity κ measured as a function of temperature for $ThGe_2$ and for single-crystal UGe_2 along the three main crystallographic directions, together with an average over the three directions (dashed curve).

the averaged thermal conductivity taken over the three (**a**, **b** and **c**) crystallographic axes. In addition, in this figure, we have plotted the thermal conductivity data for the polycrystalline sample $ThGe_2$, as a reference non-magnetic compound. In the paramagnetic region, the total thermal conductivity κ of UGe_2 measured for the temperature gradient ΔT parallel to the **a** and **c** axes decreases slightly with decreasing temperature. At the same time, this quantity along the **b** axis goes through a very broad maximum around 100 K. All three of these curves show a small drop in $\kappa(T)$ at T_C, especially seen along the **a** and **c** directions. Also along these two directions, instead of decreasing further to zero at $T = 0$ K, $\kappa(T)$ first grows markedly and then passes through a maximum near the characteristic temperature T^*, below which it starts to fall towards zero at $T = 0$ K. Such behaviour is not so apparent for the **b** axis and so marked changes in $\kappa(T)$ are not seen there at either of these characteristic temperatures. The averaged thermal conductivity also presents a small drop at T_C and a very weak maximum at T^*, but in fact these two temperatures are much more visible along the **a** and **c** directions than along the **b** direction or for the averaged value. It is also interesting to note that the averaged conductivity for UGe_2 and that of $ThGe_2$ are close to each other, which will make the determination of the magnetic contribution relatively unreliable for UGe_2.

According to expectations, $\kappa(T)$ measured for $ThGe_2$ decreases smoothly when the temperature is decreased. At first it changes slowly, but below about 50 K, $\kappa(T)$ falls much faster, as shown in figure 1. The character of the $\kappa(T)$ curve is here similar to those found for REM_3 compounds in the paramagnetic region of temperature [10]. In order to observe in more detail the temperature variations of κ at lower temperatures, we have plotted in figure 2 the $\kappa(T)$ curves for both $ThGe_2$ and UGe_2 on double-logarithmic scales. It appears that the low temperature variations of κ for all four cases can be presented as T^n, where $n < 1$ for the **a**, **b** and **c** axes of UGe_2 and $n > 1$ for $ThGe_2$. It is clear that the behaviour of κ at low temperatures follows different power laws in UGe_2 and in $ThGe_2$; however, we cannot, at present, interpret these different values of the exponent n. On the other hand, figures 1 and 2 indicate clearly the location of the two temperatures T^* and T_C and the shallow minimum observed in $\kappa(T)$ for UGe_2 between T^* and T_C. For the hard magnetization direction **b**, the anomalies at these temperatures are much more marked in figure 2 than in figure 1.

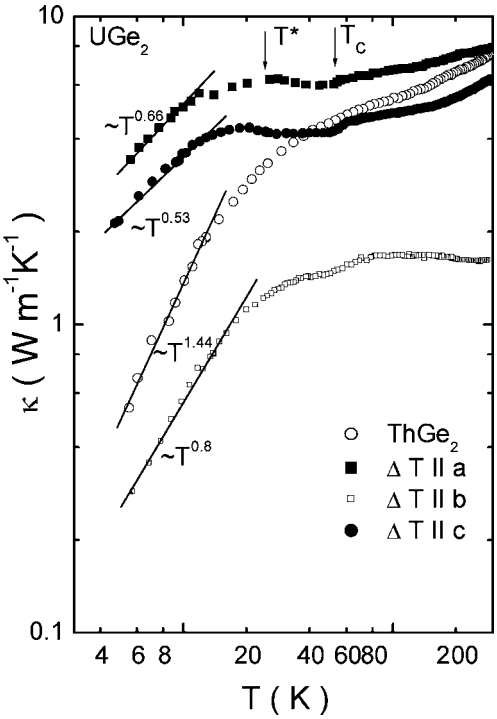

Figure 2. The thermal conductivity κ as a function of temperature for $ThGe_2$ and single-crystal UGe_2 on a double-logarithmic scale.

Figure 3 shows clearly a huge anisotropy in the thermal conductivity of UGe_2 measured along the three different axes, where the corresponding ratios κ_a/κ_c, κ_a/κ_b and κ_c/κ_b were plotted against temperature. As can be seen, the two latter ratios especially can reach at low temperatures the unusually high values of 9–11. On the other hand, in the temperature range above T_C, for example, the variation of κ_a/κ_c is almost constant with temperature, while the two other ratios are only slightly dependent on temperature. Generally, there is a marked anisotropy in the transport properties of many cerium or related compounds, but this anisotropy is much smaller than that seen here. Probably a large part of this large anisotropy comes from the orthorhombic crystal structure of UGe_2 itself. But certainly, also, below T_C, the observed strong anisotropy is connected to the almost Ising-type [4, 6] magnetic order of UGe_2, as well as to a probable difference in distribution of impurities and dislocations, depending on the heat current flow direction.

4. Discussion of the experimental results

The first very interesting result which comes from figure 1 is the very clear evidence for the two temperatures T^* and T_C. In that regard, the thermal conductivity plots along the two easy magnetization axes **a** and **c** offer a very good determination of these two magnetic temperatures, like the previous TMR experiments [6]. Thus, a large part of the thermal conductivity at low temperatures is certainly due to magnetism and in particular to the ferromagnetic order. However, considering the thermal conductivity of a magnetic material such as UGe_2 is quite difficult, because there are several contributions which enter either the thermal conductivity,

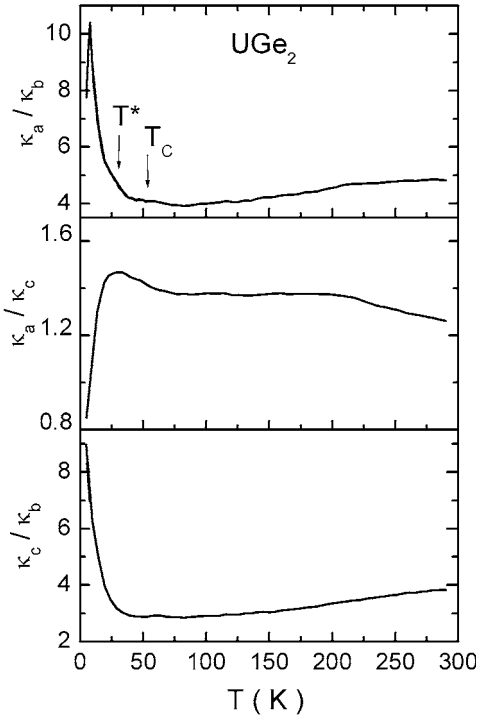

Figure 3. Anisotropy behaviour presented as the temperature dependences of the corresponding ratios of the thermal conductivities measured along the given crystallographic directions.

if they come from different carriers, or the 'thermal resistivity', for carriers of a given type scattered by different scattering mechanisms. In some special cases of strongly correlated electron systems, the Kondo or heavy fermion contribution is by far the most important one, for example for $YbAgCu_4$ [11] or $PrSn_3$ [12], and there we can directly study the behaviour of the magnetic thermal resistivity. However, as we will see below, our present case of UGe_2 does not belong to this relatively simple group and we will present here our analysis of the measurements, treating it as preliminary.

In our case of UGe_2, the analysis of the data seems to be more complicated, since the phonon and magnetic contributions to the thermal conductivity are typically of the same order of magnitude. This idea is supported primarily by the fact that the thermal conductivity of UGe_2 is relatively close to that of $ThGe_2$, especially along the **a** and **c** axes and for the averaged case. We can also say that the decrease of the magnetic electrical resistivity, indicative of the Kondo effect, is relatively small above T_C, especially along the **b** axis, where the thermal conductivity is smaller than those along the two other axes. Thus, UGe_2 is ferromagnetic below T_C, even showing a peculiar behaviour below T^*, and has a very weak Kondo behaviour above T_C, as primarily shown by resistivity measurements.

Let us however discuss in general the origin of the different contributions to the thermal conductivity for a magnetic material such as UGe_2. The total thermal conductivity may be regarded in general as a sum of three contributions:

$$\kappa = \kappa_e + \kappa_{ph} + \kappa_m \tag{1}$$

where κ_e, κ_{ph}, κ_m are electronic, phonon and magnon thermal conductivities, respectively (e.g. see [13]).

Assuming that all the above scattering mechanisms responsible for the thermal resistivity W_e are additive (according to the Matthiessen rule), the electronic contribution to the thermal conductivity can be expressed as follows:

$$\kappa_e^{-1} = W_e = W_{e,i} + W_{e,ph} + W_{e,m}. \tag{2}$$

The particular terms occurring in the above equation denote the thermal resistivity due to collisions of the conduction electrons with lattice imperfections, phonons and magnons respectively.

A similar formula can also be written for the phonon component of the thermal conductivity:

$$\kappa_{ph}^{-1} = W_{ph} = W_{ph,i} + W_{ph,e} + W_{ph,ph} + W_{ph,m} \tag{3}$$

where the terms characterize scattering of phonons on impurities and defects, conduction electrons, lattice vibrations and magnons, respectively. The scattering of electrons and phonons on the lattice imperfections, especially magnetic ones, is elastic and this mechanism is probably the most important at low temperatures. In contrast, the electron–phonon and phonon–phonon interactions may have an elastic as well as an inelastic character and thus they are described in terms of processes of normal and Umklapp types [14], respectively.

The third contribution to the thermal conductivity (see equation (1)), the magnon component κ_m, is expected to appear in the magnetically ordered state, here below the ordering temperature $T_C = 53$ K. At low temperatures the magnon and phonon contributions to the total thermal conductivity are supposed to be of comparable magnitudes. With increasing temperature the value of the ratio κ_m/κ_{ph} usually strongly decreases and becomes close to zero in the vicinity of the magnetic phase transition.

We realize that the Wiedemann–Franz (WF) law should be treated here with some caution; nevertheless, we used it below to obtain a crude estimate of the electronic part of the thermal conductivity. Assuming a relation between the thermal conductivity and electrical resistivity given by the law $L_0 = \kappa_e \rho / T$ ($L_0 = 2.45 \times 10^{-8}$ W Ω K^{-2} is the Sommerfeld constant), we derived the expected temperature variation of the electronic contribution to the total thermal conductivity (not shown here), measured in the three main orthorhombic directions of UGe_2. In this procedure, the electrical resistivity data were taken from [6], taking care that the electrical resistivity and thermal conductivity measurements were performed on the same single-crystalline sample. On this basis we were able to deduce that κ_e in all the three directions decreases almost linearly with decreasing temperature; then at T_C it starts to rise, at first slowly; and then, below T^*, κ_e increases suddenly to 1–6 W mK^{-1}, depending on the particular crystallographic direction. This observation is in fairly good agreement with the results on the Hall effect $R_H(T)$, recently studied for a single-crystalline sample of UGe_2 [15]. In this study the charge carrier density was found to increase rapidly just below T^*, suggesting some Fermi surface reconstruction. The above analysis of course could be quite correct if L were to be actually equal to L_0. In figure 4 we have plotted the reduced ratio L/L_0 as a function of temperature for the three crystallographic directions of UGe_2 and also for $ThGe_2$. We see immediately that L is quite different from L_0, depending strongly on temperature, and therefore one must be doubtful of the previous analysis of the values of κ_e.

In the case of $ThGe_2$, $\rho(T)$ shows typical metallic character (see figure 5). For this compound the ratio L/L_0 above about 20 K is kept constant up to room temperature, being only slightly enhanced to a value of 1.6. On the other hand, the reduced Lorenz number L/L_0 for UGe_2 varies strongly with temperature along the three axes and reaches near T_C maximum values of 5–7 times higher than the Sommerfeld number L_0. At the same time, this ratio even drops below 1 at the lowest temperature measured, as shown in figure 4, and is still higher than 1 at room temperature for all the crystallographic directions studied.

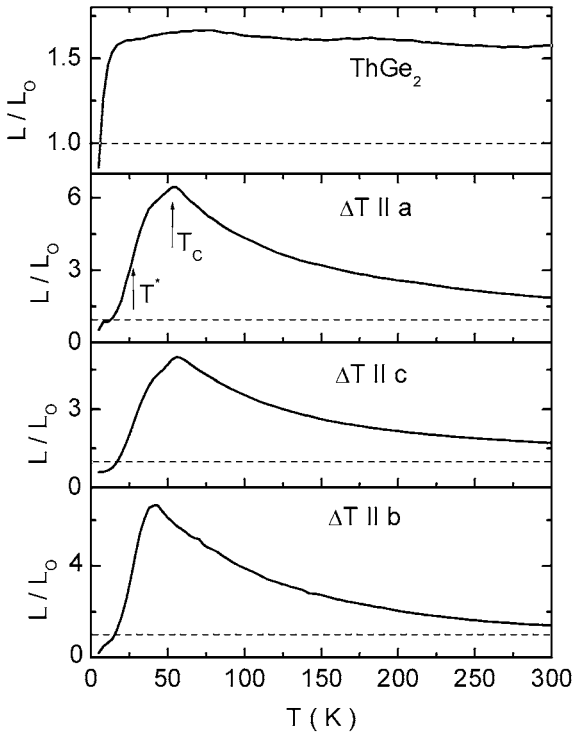

Figure 4. The reduced Lorenz ratio L/L_0 as a function of temperature calculated for bulk $ThGe_2$ and a single crystal of UGe_2 along the three crystallographic directions.

For UGe_2, which can be regarded as a semimetal, the phonon contribution κ_{ph} to the thermal conductivity is expected to increase when the temperature is lowered. We can only conjecture that the large L/L_0 values near T_C are caused primarily by domination of the phonon scattering in the vicinity of this critical temperature. At higher temperatures, both the anharmonic phonon–phonon collisions (U processes) and the scattering on the disordered magnetic moments decrease the phonon part of the contribution in $\kappa(T)$, while $\kappa_e(T)$ above T_C increases probably linearly with temperature, in a manner similar to that reported e.g. for UPd_2Al_3, above T_N [16].

We finally present here an alternative attempt at an explanation of the results in order to determine the magnetic contribution in the thermal conductivity of UGe_2, based on a comparison with the case of $ThGe_2$. The following procedure could be criticized because the averaged thermal conductivity of UGe_2 is close to that of $ThGe_2$ and consequently we cannot use the averaged value to perform the following analysis. Practically, our analysis was possible only for the **b** hard axis for which the $\kappa(T)$ curve runs considerably lower than that for $ThGe_2$ (see figure 1), but paradoxically the Kondo effect observed in the resistivity data (see figure 5) is much smaller along the **b** axis than along the two other axes (see figure 2 in [6]). Thus, we define $\Delta W = W_b(UGe_2) - W(ThGe_2)$, where W_b is the thermal resistivity measured along the **b** axis, as a 'magnetic contribution' and we plot in figure 6 the product $\Delta W^* T$ against $\ln T$. If we anticipate the following analysis, we see immediately in figure 6 that the resulting $\Delta W^* T$ deduced by taking the averaged conductivity of UGe_2 is negligible. This figure shows first an increase of $\Delta W^* T$ above T_C, in contradiction to the decrease observed in the case of a strong Kondo effect [12]. However, we can also see in figure 5, where we

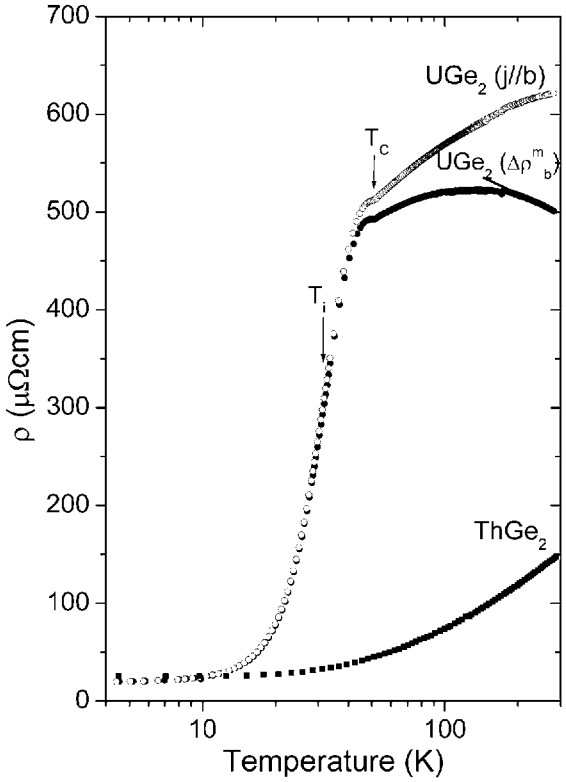

Figure 5. The electrical resistivity ρ versus $\log T$ for a bulk $ThGe_2$ and a single crystal of UGe_2 measured along the hard axis **b**. In addition there is also shown the temperature dependence of the difference $\Delta\rho_b^{\mathrm{m}}$ in the resistivities of UGe_2, measured along the **b** axis, and $ThGe_2$. T_i is an inflection point.

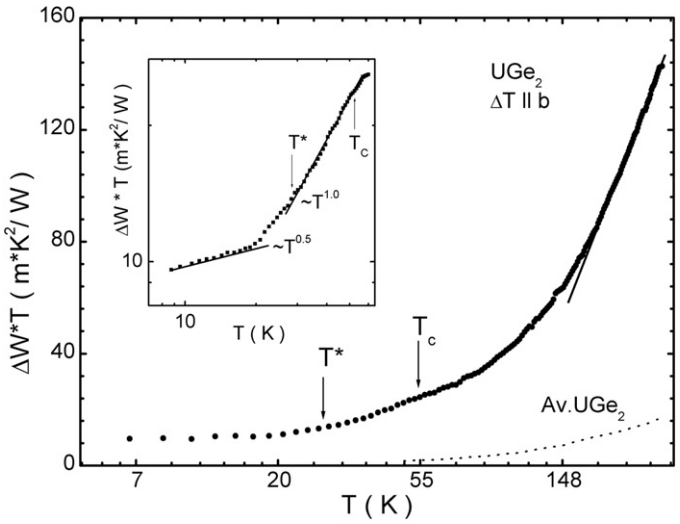

Figure 6. The product $\Delta W^* T$ versus $\ln T$ derived for the hard **b** direction and for the case of an average over the three directions (dashed curve). The temperature dependence for the hard **b** direction is also shown in the inset on a double-logarithmic scale for temperatures below T_C.

have plotted the resistivity of $ThGe_2$ and also the difference between the resistivities along the **b** axes of UGe_2 and $ThGe_2$ against $\log T$, that the Kondo effect is almost invisible above T_C for the resistivity along the hard axis **b**. Thus, figure 6 shows clearly a sudden decrease of the magnetic contribution in the thermal conductivity with decreasing temperature below room temperature with the $\ln T$ dependence in the paramagnetic region down to roughly 160 K. In the inset of this figure the double-logarithmic plot of $\Delta W^* T$ versus T is presented in the temperature region below T_C. On this basis we have found a T^n dependence below and above the characteristic temperature T^* with the exponents n given in the figure and a change in the value of this exponent is observed at this characteristic temperature. Only a further study using a strong magnetic field and high pressure will allow us to explain all these thermal behaviours of the heat transport in UGe_2.

5. Conclusions

We have performed measurements of the thermal conductivity and electrical resistivity for polycrystalline $ThGe_2$ and single-crystalline UGe_2 in the temperature region 4.2–300 K. Both these quantities for UGe_2 are strongly anisotropic in their temperature variations, depending on the crystallographic directions. Distinct anomalies at T_C and T^* are observed in the plots of the thermal conductivity, exactly as seen previously in the TMR plots. Also we observed a large increase in the reduced Lorenz number L/L_0 in the vicinity of T_C for all three crystallographic directions of UGe_2. Below T_C, but especially below T^*, we observed the steep decrease in the L/L_0 ratio down to 1 or even less, originating from the steep fall of the resistivity [6], which points to a considerable increase of the electron contribution to κ and a sudden decrease in the phonon contribution. The thermal conductivity measured for $ThGe_2$ has allowed us to separate out a possible 'magnetic part' of the thermal resistivity ΔW of UGe_2 along the hard direction **b** and we can conclude that the Kondo effect is very weak in UGe_2 if we consider the magnetic parts of the thermal resistivity and the electrical resistivity.

Finally, the present experiments give clear evidence for the two temperatures T_C and T^* and show that the Kondo effect is very weak. However, the theoretical separation of the different contributions to the thermal conductivity remains a difficult challenge, as does the coexistence between superconductivity, ferromagnetism and a weak Kondo effect observed in UGe_2.

Acknowledgments

The authors are grateful to Professor T Komatsubara for his help in obtaining single crystals of UGe_2. The work was partly supported by a KBN Grant No 2P03B 109 24.

References

[1] See a vast review: Huxley A, Sheikin I, Ressouche E, Kernavanois N, Braithwaite D, Calemczuk R and Flouquet J 2001 *Phys. Rev.* B **63** 144519 and references therein
[2] Oomi G, Kagayama Y and Onuki Y 1998 *J. Alloys Compounds* **271–273** 482
[3] Oomi G, Ohashi M, Nishimura K and Onuki Y 2002 *J. Nucl. Sci. Technol.* **3** (Suppl.) 90
[4] Menovsky A, de Boer F R, Frings P H and France J J M 1983 *High Field Magnetism* ed M Date (Amsterdam: North-Holland) p 189
[5] Troć R, Noël H and Boulet P 2002 *Phil. Mag.* B **82** 805
[6] Troć R 2003 *Acta Phys. Pol.* B **34** 407
[7] Boulet P, Daudi A, Potel M, Noël H, Gross G M, Andre G and Bouree F 1997 *J. Alloys Compounds* **247** 104
[8] Brown A 1962 *Acta Crystallogr.* **15** 652

[9] Jeżowski A, Mucha J and Pompe G 1987 *J. Phys. D: Appl. Phys.* **20** 1500
[10] Smirnov I A and Oskotski V S 1993 *Thermal Conductivity of Rare Earth Compounds* (*Handbook on Physics and Chemistry of Rare Earths* vol 16) ed K A Gschneidner (Amsterdam: Elsevier)
[11] Bauer E, Gratz E, Hutflesz G, Bhattacharjee A K and Coqblin B 1992 *J. Magn. Magn. Mater.* **108** 159
Bauer E, Gratz E, Hutflesz G, Bhattacharjee A K and Coqblin B 1993 *Physica* B **186–188** 494
[12] Kletowski Z, Mucha J, Misiorek H, Onuki Y and Coqblin B 2004 *J. Magn. Magn. Mater.* **272–276** e97
[13] Mucha J, Misiorek H, Kaczorowski D and Jeżowski A 1992 *J. Alloys Compounds* **189** 217
[14] Berman R 1976 *Thermal Conductivity in Solids* (Oxford: Clarendon)
[15] Tran V H, Paschen S, Troć R, Baenitz M and Steglich F 2004 *Phys. Rev.* B **69** 195314
[16] Hiroi M, Sera M, Kobayasshi N, Haga Y, Yamamoto E and Onuki Y 1997 *J. Phys. Soc. Japan* **66** 1595